Materials Letters 188 (2017) 271–274

Contents lists available at ScienceDirect

Materials Letters

journal homepage: www.elsevier.com/locate/matlet

$CH_3NH_3PbI_3$ thin films prepared by pulsed laser deposition for optoelectronic applications

Dandan Liu[a], Xueliu Li[a], Chengwu Shi[b,*], Qi Liang[a,*]

[a] School of Electronic Science & Applied Physics, Hefei University of Technology, Hefei, Anhui 230009, PR China
[b] School of Chemistry and Chemical Engineering, Hefei University of Technology, Hefei, Anhui 230009, PR China

ARTICLE INFO

Keywords:
Perovskite $CH_3NH_3PbI_3$
Thin films
Semiconductors
Deposition
Heterojunction

ABSTRACT

$CH_3NH_3PbI_3$ thin films were prepared on glass substrates by pulsed laser deposition. The phase structural properties of the films deposited with different pulse repetition rates were analyzed carefully. The films deposited at 8 Hz and other rates show a single phase $CH_3NH_3PbI_3$ and mixed $CH_3NH_3PbI_3$-PbI_2 phases, respectively. The prepared $CH_3NH_3PbI_3$ film possesses absorption coefficients of 10^4 cm^{-1} in the visible region and the optical band gap of 1.66 eV. The $CH_3NH_3PbI_3$/n-Si heterojunction device was fabricated. The I-V characteristics of the heterojunction in the dark and under illumination exhibit good rectifying behavior and fast photoresponse. The rise and fall time of the device were measured to be 58.8 μs and 1.9 μs.

1. Introduction

The hybrid organic-inorganic perovskite materials as promising light harvesters, such as $CH_3NH_3PbI_3$, have attracted great attention in research on photovoltaic and optoelectronic devices due to their excellent optical and electronic properties [1]. $CH_3NH_3PbI_3$ possesses some superior properties, such as a favourable direct band gap, high absorption coefficients, high carrier mobilities and long carrier-diffusion lengths for both electrons and holes [2]. Preparation methods of $CH_3NH_3PbI_3$ include spin-coating [3], two-step chemical solution deposition [4], dual-source evaporation [5] and so on. The pulsed laser deposition (PLD) is a technique for growing high quality thin films and being suitable for investigating basic properties of thin films. The technique features energetic and non-equilibrium processes with precise preparation parameter control, forming stoichiometric films with high crystallinity. The literature [6] studied the growth of $CH_3NH_3PbI_{3-x}A_x$ (A=Cl or F) films by off-axis deposition of PLD. Although no more reports on hybrid perovskite films deposited by PLD have been found to date, the interests on this topic will be expected. Nowadays, photodetectors based on novel semiconductor materials, including hybrid perovskites, have gained great interests [7–10], and heterojunctions may be a promising strategy because of their superior device characteristics and simple device structures [10,11]. In this work, we have prepared $CH_3NH_3PbI_3$ films by on-axis deposition of PLD and fabricated a $CH_3NH_3PbI_3$/n-Si heterojunction device, investigating the structural and optical properties of $CH_3NH_3PbI_3$ films and the optoelectric characteristics of the device.

2. Experimental method

2.1. Preparation of $CH_3NH_3PbI_3$ films

$CH_3NH_3PbI_3$ thin films were deposited on glass substrates by PLD (on-axis case) using a KrF excimer laser (COMPexPro 102, 248 nm, 25 ns) at room temperature. The target was made by mixing the PbI_2 and CH_3NH_3I in mole ratio of 1:10 and pressing it under 40 MPa. The substrates were placed 5 cm away from the target. The laser fluence is 0.4 J/cm^2. The deposition chamber was evacuated to a base pressure of 4.0×10^{-4} Pa. The pulse repetition rate was set to be 2 Hz, 5 Hz, 8 Hz and 11 Hz for sample S1, S2, S3 and S4, respectively. And correspondingly, the deposition time was 100 min, 40 min, 25 min and 18 min, respectively, for the number of pulse remaining constant (12,000 pulses).

2.2. Fabrication of device

The architecture of Au/$CH_3NH_3PbI_3$/n-Si/Au device is shown in Fig. 3(a). $CH_3NH_3PbI_3$ layer (~600 nm) was deposited on the n-type Si substrate with the resistivity of 1–10 Ω cm by PLD at 8 Hz for 25 min. The Au electrodes (~50 nm) were prepared on $CH_3NH_3PbI_3$/n-Si heterojunction by electron beam evaporation with base pressure of 5×10^{-3} Pa.

2.3. Characterizations

The crystalline structure of $CH_3NH_3PbI_3$ thin films was studied by

* Corresponding authors.

http://dx.doi.org/10.1016/j.matlet.2016.10.113
Received 30 August 2016; Received in revised form 20 October 2016; Accepted 30 October 2016
Available online 01 November 2016

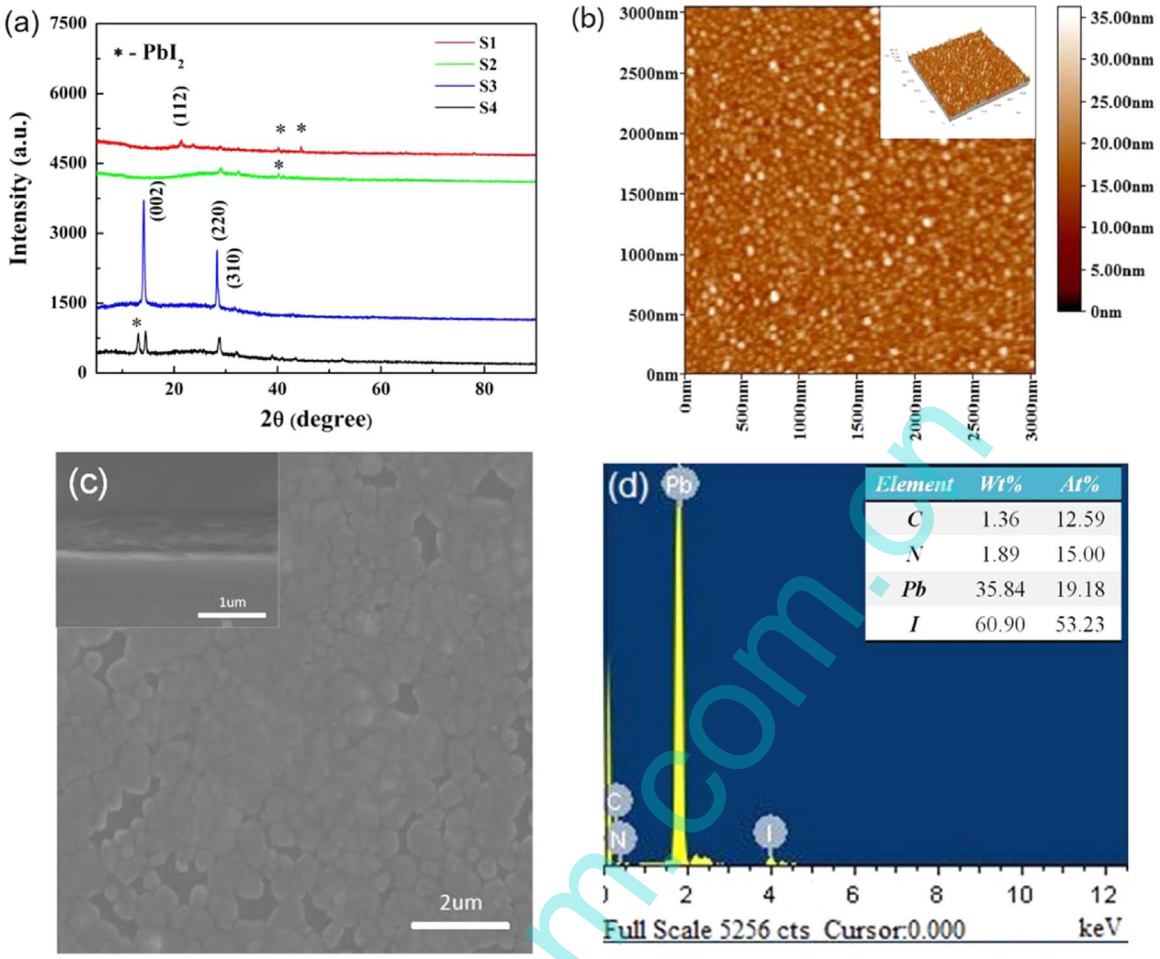

Fig. 1. (a) XRD patterns of $CH_3NH_3PbI_3$ films prepared at different pulse repetition rates. (b) AFM image, (c) SEM image and (d) EDS spectrum of sample S3.

an X-ray diffractometer (D/MAX2500, Rigaku, Cu Kα). The Raman and photoluminescence (PL) spectrum were recorded using a spectrometer (Horiba Yvon Jobin) equipped with a solid state laser with an excitation wavelength of 532 nm. A scanning electron microscope (FE-SEM, Sirion200) and an atomic force microscope (AFM, CSPM4000) were used to measure the morphologies. Chemical compositions were determined by energy dispersive X-ray spectroscopy (EDS, JSM-6490LV). The optical properties were measured by a UV–VIS–NIR spectrophotometer (Cary5000). Current-voltage (I-V) characteristics of the device were measured using a semiconductor characterization system (Keithley 4200-SCS).

3. Results and discussion

3.1. Structural analysis

The X-Ray Diffraction (XRD) spectra of $CH_3NH_3PbI_3$ films deposited with different pulse repetition rates (sample S1-S4) are shown in Fig. 1(a). It is found that all the prepared films are crystallized, but differ greatly in crystallinity. Four diffraction peaks are found at 2θ=14.13°, 21.45°, 28.33°, and 31.75° corresponding to the (002), (112), (220) and (310) planes of $CH_3NH_3PbI_3$, which are good in agreement with the previous reports [2,12]. Moreover, the impurity peaks are also found at 13.10°, 40.20° and 44.56° which can be attributed to PbI_2 crystals in S1, S2 and S4. For S1, two peaks of PbI_2 emerge in addition to the (112) and (220) peaks of $CH_3NH_3PbI_3$. For S2, there are two peaks corresponding to $CH_3NH_3PbI_3$ (220) and (310) planes, and one peak of PbI_2 also appears. Both S1 and S2 have poor crystallinity due to the low intensity of the diffraction peaks, being composed of $CH_3NH_3PbI_3$ and PbI_2 phases. For S4, the (002) and (220) peaks of $CH_3NH_3PbI_3$ appear, with higher intensity compared with the signal in S1 and S2, but the peak of PbI_2 is also contained. For the film of S3 deposited at 8 Hz, the (002), (220) and (310) peaks can be well matched with tetragonal phase of $CH_3NH_3PbI_3$ [12]. The film has the lattice parameters of a=8.904 Å, c=12.526 Å, and α=β=γ=90°. The intensity of (002) and (220) peaks is rather high, which indicates S3 is polycrystalline with high crystallinity. And the sample is aligned along (002) preferred orientation. The above results indicate influence of the pulse repetition rate on crystallinity and phase purity of $CH_3NH_3PbI_3$ films. The difference in phase structure and crystallinity for sample S1-S4 depends on the interval of arriving pulses and the balance of reevaporation of organic and inorganic components. The single phase $CH_3NH_3PbI_3$ film possesses a favourable band gap and excellent light absorption ability, but in the case of mixed $CH_3NH_3PbI_3$-PbI_2 phases, the band gap increases and light absorption weakens because of existence of PbI_2 phase.

The Raman spectrum for the film (sample S3) is shown in Fig. 2(a), and there are two intense Raman peaks belonging to $CH_3NH_3PbI_3$ located at 93.4 and 108.0 cm^{-1}, respectively [13,14]. The result of Raman analysis matches with the XRD observations and further confirms that the film is a single phase perovskite $CH_3NH_3PbI_3$.

3.2. Surface morphological and compositional analysis

The morphologies of $CH_3NH_3PbI_3$ film of sample S3 were analyzed with AFM and SEM. Fig. 1(b) shows the 2D and 3D AFM images of the film. The surface morphology of the film as observed from the AFM images proves that the grains are uniform in size and in distribution,

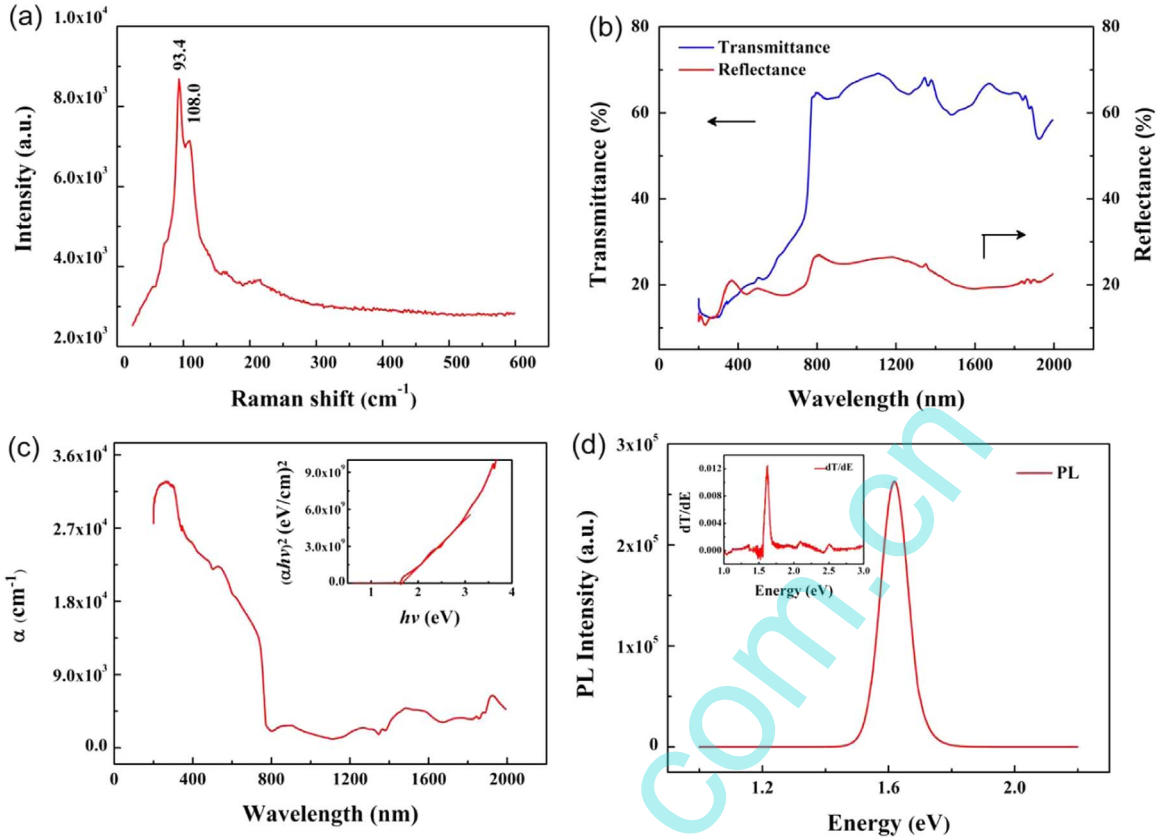

Fig. 2. (a) Raman spectrum, (b) Transmittance and Reflectance spectra of Sample S3. (c) The absorption coefficient α of S3, and a plot of $(\alpha h\nu)^2$ vs hν (inset). (d) Photoluminescence spectrum of S3 and the inset shows plot of the derivative of the transmittance with respect to energy of S3.

and the average grain size is 81.9 nm. The average roughness is 2.23 nm. The top view and cross-sectional SEM images of $CH_3NH_3PbI_3$ film are shown in Fig. 1(c). It can be observed that the film is composed of homogeneous plate-like crystallites and densely covered. The cross-sectional image confirms a compact morphology and a uniform film thickness of 600 nm. The elemental compositions of the $CH_3NH_3PbI_3$ film analyzed using EDS are shown in Fig. 1(d). The result shows the composition of C, N, Pb and I elements present at a nearly stoichiometric atomic ratio of 12.59, 15.00, 19.18 and 53.23, respectively.

3.3. Optical properties

The transmittance and reflectance spectra of the $CH_3NH_3PbI_3$ thin film (sample S3) are shown in Fig. 2(b). The absorption coefficient (α) of the film, shown in Fig. 2(c), is calculated from the transmittance and reflectance spectra using the equation $\alpha=\ln((1-R)/T)/d$, where d is the thickness of the film [15]. The value of α at 600 nm is 1.8×10^4 cm^{-1}, which signifies the light harvesting capability of the perovskite in the visible region of the spectrum. Additionally, the value of the optical band gap can be determined from the standard relation [12]. The band gap of 1.66 eV can be obtained from extrapolation of the linear region in the Tauc plot, $(\alpha h\nu)^2$ versus energy, as shown in the inset of Fig. 2(c). The PL spectrum of the $CH_3NH_3PbI_3$ film is shown in Fig. 2(d). The PL spectrum exhibits the only one intense emission peak at around 1.62 eV (766.12 nm) corresponding to the band gap of the film. Furthermore, the band gap of the thin film can be determined from the position of the maximum of first derivative of the optical transmittance (dT/dE), as shown in inset of Fig. 2(d), and the as determined band gap is 1.62 eV.

3.4. Device performances

Fig. 3(b) and (c) show the I-V characteristics of the $CH_3NH_3PbI_3$/n-Si heterojunction in the dark and under various illumination intensities. The illumination wavelength is 650 nm. The dark I-V characteristic of the device exhibits a good rectifying behavior. The insets of Fig. 3(b) indicate that Au electrodes form ohmic contacts with Si and $CH_3NH_3PbI_3$ film, respectively. As seen in Fig. 3(c), both the forward and reverse current increase under illumination ranging from 2.5 to 35.6 mW/cm^2 to confirm that the device show considerable photocurrent response. Fig. 3(d) shows the photoresponse of the $CH_3NH_3PbI_3$/n-Si heterojunction to pulsed light with frequency of 900 Hz and 50 kHz, manifesting that the device can work well even for high frequency (50 kHz) optical signals. In addition, from the enlarged photoresponse curve at 900 Hz, as shown in Fig. 3(d), the rise and the fall time are measured to be 58.8 μs and 1.9 μs, respectively. This response speed is faster than other reported $CH_3NH_3PbI_3$-based photodetectors [7,8], and near the perovskite $MAPbBr_3$-based photodetector [9] and the MoS_2-based high speed photodetectors [10].

4. Conclusions

High quality $CH_3NH_3PbI_3$ films have been deposited successfully by pulsed laser deposition. The $CH_3NH_3PbI_3$ film grown at the pulse repetition rate of 8 Hz with a laser fluence of 0.4 J/cm^2 has high crystallinity and good light harvesting capability with the optical band gap of 1.66 eV. The I-V characteristics of the $CH_3NH_3PbI_3$/n-Si heterojunction show good rectification property. The photoelectric characteristics and fast photoresponse of the device indicate $CH_3NH_3PbI_3$ films' promising applicability for high performance photoelectric devices.

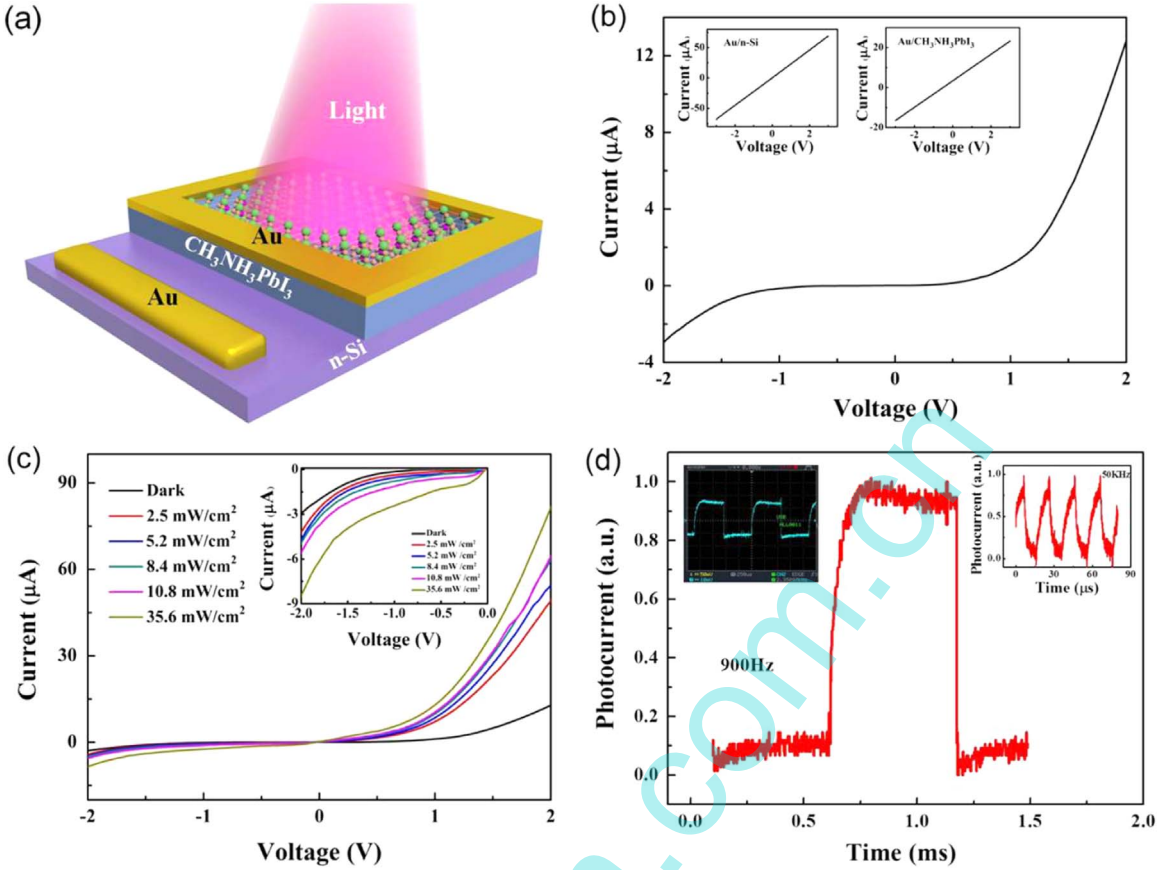

Fig. 3. (a) Schematic illustration of a $CH_3NH_3PbI_3$/n-Si heterojunction-based photodetector. (b) I-V characteristics of the $CH_3NH_3PbI_3$/n-Si heterojunction under dark condition, the inset is I-V characteristic of Au/n-Si and Au/$CH_3NH_3PbI_3$ structure. (c) I-V curves of the $CH_3NH_3PbI_3$/n-Si heterojunction under various illumination intensities, the inset shows the details in the reverse bias region. (d) One normalized cycle of photocurrent response of device under pulsed light illumination (650 nm) measured at 900 Hz for estimating both rise time (τ_r) and fall time (τ_f). The left inset is the oscilloscope figure of photoresponse characteristics at 900 Hz, the right inset is the plot of photoresponse at 50 kHz.

Acknowledgements

This work was supported by the National Natural Science Foundation of China (No. 51472071).

References

[1] Z.W. Gu, F. Chen, X.Q. Zhang, Y.J. Liu, et al., Sol. Energy Mat. Sol. C 140 (2015) 396–404.
[2] Y.Y. Zhou, M.J. Yang, A.L. Vasiliev, H.F. Garces, et al., J. Mater. Chem. A 3 (2015) 9249–9256.
[3] M.H. Zulkifli, A. Bahtiar, AIP Conf. Proc. 1712 (2016) (050012/1-5).
[4] Q. Chen, H.P. Zhou, Z.R. Hong, S. Luo, et al., J. Am. Chem. Soc. 136 (2014) 622–625.
[5] P. Fan, D. Gu, G.X. Liang, J.L. Chen, et al., J. Mater. Sci: Mater. Electron 27 (2016) 2321–2327.
[6] U. Bansode, R. Naphade, O. Game, S. Agarkar, et al., J. Phys. Chem. C 119 (2015) 9177–9185.
[7] C. Zhu, Y. Tang, F. Chen, A. Gowri Manohari, et al., J. Cryst. Growth 454 (2016) 121–127.
[8] L. Su, Z.X. Zhao, H.Y. Li, J. Yuan, et al., ACS Nano 9 (2015) 11310–11316.
[9] M.I. Saidaminov, V. Adinolfi, R. Comin, et al., Nat. Commun. 6 (2015) 9724.
[10] Y. Zhang, Y.Q. Yu, L.F. Mi, H. Wang, Z.F. Zhu, et al., Small (8) (2016) 1062–1071.
[11] J. Mao, Y.Q. Yu, L. Wang, X.J. Zhang, et al., Adv. Sci. (2016) (1600018/1-9).
[12] P. Bhatt, K. Pandey, P. Yadav, B. Tripathi, et al., Sol. Energy Mat. Sol. C 140 (2015) 320–327.
[13] C. Quarti, G. Grancini, E. Mosconi, P. Bruno, et al., J. Phys. Chem. Lett. 5 (2014) 279–284.
[14] R. Gottesman, L. Gouda, B.S. Kalanoor, et al., J. Phys. Chem. Lett. 6 (2015) 2332–2338.
[15] F.Y. Ran, Z. Xiao, H. Hiramatsu, H. Hosono, et al., Appl. Phys. Lett. 104 (2014) (072106/1-4).